



# The Effects of Terminal Tagging on Homomeric Interactions of the Sigma 1 Receptor

Hideaki Yano\*, Leanne Liu, Sett Naing and Lei Shi\*

Computational Chemistry and Molecular Biophysics Unit, National Institute on Drug Abuse – Intramural Research Program, National Institutes of Health, Baltimore, MD, United States

## OPEN ACCESS

### Edited by:

Said Kourrich,  
Université du Québec à Montréal,  
Canada

### Reviewed by:

Lianwang Guo,  
The Ohio State University,  
United States  
Robert B. Laprairie,  
University of Saskatchewan, Canada

### \*Correspondence:

Hideaki Yano  
hideaki.yano@nih.gov  
Lei Shi  
lei.shi2@nih.gov

### Specialty section:

This article was submitted to  
Neuropharmacology,  
a section of the journal  
Frontiers in Neuroscience

**Received:** 14 August 2019

**Accepted:** 02 December 2019

**Published:** 19 December 2019

### Citation:

Yano H, Liu L, Naing S and Shi L  
(2019) The Effects of Terminal Tagging  
on Homomeric Interactions of the  
Sigma 1 Receptor.  
*Front. Neurosci.* 13:1356.  
doi: 10.3389/fnins.2019.01356

The sigma 1 receptor ( $\sigma$ 1R) has been implicated in cancers, neurological disorders, and substance use disorders. Yet, its molecular and cellular functions have not been well-understood. Recent crystal structures of  $\sigma$ 1R reveal a single N-terminal transmembrane segment and C-terminal ligand-binding domain, and a trimeric organization. Nevertheless, outstanding issues surrounding the functional or pharmacological relevance of  $\sigma$ 1R oligomerization remain, such as the minimal protomeric unit and the differentially altered oligomerization states by different classes of ligands. Western blot (WB) assays have been widely used to investigate protein oligomerizations. However, the unique topology of  $\sigma$ 1R renders several intertwined challenges in WB. Here we describe a WB protocol without temperature denaturation to study the ligand binding effects on the oligomerization state of  $\sigma$ 1R. Using this approach, we observed unexpected ladder-like incremental migration pattern of  $\sigma$ 1R, demonstrating preserved homomeric interactions in the detergent environment. We compared the migration patterns of intact  $\sigma$ 1R construct and the C-terminally tagged  $\sigma$ 1R constructs, and found similar trends in response to drug treatments. In contrast, N-terminally tagged  $\sigma$ 1R constructs show opposite trends to that of the intact construct, suggesting distorted elicitation of the ligand binding effects on oligomerization. Together, our findings indicate that the N-terminus plays an important role in eliciting the impacts of bound ligands, whereas the C-terminus is amenable for modifications for biochemical studies.

**Keywords:** sigma 1 receptor, western blot, oligomerization, bioluminescence resonance energy transfer, SDS-PAGE

## INTRODUCTION

The sigma 1 receptor ( $\sigma$ 1R) is a structurally unique transmembrane protein found in the endoplasmic reticulum (ER) and is associated with intracellular membranes in which it has been posited to act as a molecular chaperone (Su et al., 2016). Although it is broadly distributed in many different tissues and cell types, it is particularly enriched in the central nervous system (Weissman et al., 1988).  $\sigma$ 1R has been implicated in cancer, neurodegenerative diseases, and psychostimulant abuse, and is thus considered a promising therapeutic target (Maurice and Su, 2009). Despite its physiological and pharmacological significance, the structure-function relationships of  $\sigma$ 1R are poorly understood. The recent crystal structures of  $\sigma$ 1R in complexes with a variety of ligands provide the foundation for mechanistic elucidation of its function at the molecular level (Schmidt et al., 2016, 2018). They shed light on the conformation and homomeric status of

$\sigma$ 1R in the membrane environment. However, functional categorizations of  $\sigma$ 1R ligands remain challenging (Katz et al., 2017). Both the differences in intra- or extracellular environments in various  $\sigma$ 1R assays and the lack of functional readouts detecting changes in  $\sigma$ 1R itself may have contributed to the difficulty in reaching consensus conclusions. Thus, it begs the need for an assay that directly monitors changes occurring in  $\sigma$ 1R.

By focusing on  $\sigma$ 1R itself, we have developed a bioluminescence resonance energy transfer (BRET)-based assay to categorize  $\sigma$ 1R ligands based on presumed changes in  $\sigma$ 1R- $\sigma$ 1R interactions; for instance, haloperidol increases the  $\sigma$ 1R- $\sigma$ 1R interaction while (+)-pentazocine decreases it (Yano et al., 2018). However, the underlying molecular mechanism could not be directly derived from the BRET signal changes. Instead, the specific oligomerization states were characterized by western blot (WB) (Yano et al., 2018). This biochemical approach has the advantages of being capable of quantifying the sizes and intensities of migration bands to provide stoichiometric information on homomeric oligomerization, and of allowing comparison across tightly controlled experimental conditions or different pharmacological treatments. In both BRET and WB,  $\sigma$ 1R has been subjected to end tagging. However, studies have shown that a bulky protein tag on the N-terminus yields aberrant localization and function, while the C-terminal protein tagging appeared to be permissive and largely retained its function (Hayashi and Su, 2003).

In the current study, we investigated the effects of N- and C-terminal tagging on the cellular function of  $\sigma$ 1R, in particular its homomeric interactions, in order to evaluate the validity of using such constructs *in vitro* assays. We optimized a WB protocol to detect ligand-induced  $\sigma$ 1R oligomerization and compare the results for terminally tagged and unmodified wildtype (WT)  $\sigma$ 1R constructs.

## MATERIALS AND METHODS

### DNA Constructs, Transfection, and Cell Culture

HEK293T  $\Delta\sigma$ 1R cells were generated using the CRISPR-Cas9 gene deletion method (Santa Cruz). Human  $\sigma$ 1R is tagged in pcDNA3.1 plasmid with Myc, NanoLuciferase (Nluc), or mVenus, either N-terminally or C-terminally in frame without any linker (Myc- $\sigma$ 1R, Nluc- $\sigma$ 1R,  $\sigma$ 1R-Myc,  $\sigma$ 1R-Nluc, or  $\sigma$ 1R-mVenus). All constructs were confirmed by sequence analysis. For western blot and radioligand binding, 5  $\mu$ g (otherwise noted) of terminally tagged and unmodified  $\sigma$ 1R plasmid was transfected using lipofectamine 2000 (Invitrogen) for HEK 293T  $\Delta\sigma$ 1R cells in a 10 cm plate. For drug induced BRET, a constant amount of total plasmid cDNA (15  $\mu$ g) in 1:24 (donor:acceptor ratio for  $\sigma$ 1R-Nluc and  $\sigma$ 1R-mVenus) was transfected in HEK 293T  $\Delta\sigma$ 1R cells using polyethylenimine (PEI) in a 10 cm plate. Cells were maintained in culture with Dulbecco's modified Eagle's medium supplemented with 10% fetal bovine serum and kept in an incubator at 37°C and 5% CO<sub>2</sub>. Experiments were performed approximately 48 h post-transfection.

### Western Blot

HEK293T  $\Delta\sigma$ 1R cells were grown as reported (Yano et al., 2018) and transiently transfected with the unmodified  $\sigma$ 1R, N-terminally tagged Myc- $\sigma$ 1R, N-terminally tagged Nluc- $\sigma$ 1R, C-terminally tagged  $\sigma$ 1R-Myc, or C-terminally tagged  $\sigma$ 1R-Nluc in 10 cm plates. After 48 h of growth, confluent cells were harvested in Hank's Balanced Salt Solution (HBSS), centrifuged at 900  $\times$  g for 8 min, and resuspended in HBSS. The cells were then incubated in 1  $\mu$ M haloperidol, 1  $\mu$ M PD 144418, 10  $\mu$ M (+)-pentazocine, or 1% DMSO vehicle for 1 h at room temperature. The samples were then centrifuged at 900  $\times$  g for 4 min and resuspended in lysis buffer [150 mM NaCl, 1.0% triton X-100, 0.5% sodium deoxycholate, Tris 50 mM, pH 7.5, and protease inhibitors (Roche, catalog# 11697498001)]. In the case of mouse tissue preparation, a cortex was dissected out, washed in phosphate buffered saline (PBS), and homogenized in lysis buffer with tissue homogenizer. The samples were sonicated, incubated on ice for 30 min, and centrifuged at 20,000  $\times$  g for 30 min. Supernatants were transferred to new tubes. Protein concentrations of the supernatants were determined with Bradford protein assay (Bio-Rad, Hercules, CA, United States). Supernatants were mixed with 4 $\times$   $\beta$ -mercaptoethanol Laemmli sample buffer to a final 25  $\mu$ g protein/sample. Samples were electrophoresed at 100 V for 10 min (stacking gel) and 150 V for 30 min (resolving gel) on 10% polyacrylamide Tris-glycine gels (Invitrogen) with running buffer (25 mM Tris, 192 mM glycine and 0.1% SDS, pH 8.3, Invitrogen). Proteins were transferred to PVDF membranes (Invitrogen, catalog# IB24002) for 10 min at 20 V using dry transfer apparatus (Invitrogen, catalog# IB21001) and immunoblotted with antibodies in tris-buffered saline with 0.1% Tween 20. Anti-GAPDH or anti-actin was used as a loading control. The product information and dilutions of primary and secondary antibodies used are summarized in **Supplementary Table S1**. Blots were imaged using Odyssey LI-COR scanner and analyzed with LI-COR Image Studio<sup>TM</sup>. Photon counts were tabulated for each band density and normalized to the GAPDH band of the same lane. Further, those values are normalized to the summation of all band densities within the same lane as one in percent population graphs in segmented red and blue bars. Fold change bar graphs for different ligands were prepared with the photon counts (not the segmented percentage values) normalized against DMSO vehicle as mean  $\pm$  SEM.

### Radioligand Binding Assay

Membrane fraction of HEK293T  $\Delta\sigma$ 1R cells was prepared as previously described (Yano et al., 2018). The radioligand incubation was carried out in 96-well plates containing 60  $\mu$ L fresh Earle's Balanced Salts Solution (EBSS) binding buffer (8.7 g/l Earle's Balanced Salts without phenol red (United States Biological) and 2.2 g/L sodium bicarbonate, pH to 7.4), 20  $\mu$ L of (+)-pentazocine (varying concentrations), 100  $\mu$ L membranes (25  $\mu$ g/well total protein), and 20  $\mu$ L of radioligand diluted in binding buffer (1 nM [<sup>3</sup>H]-(+)-pentazocine (American Radiolabeled Chemicals), final concentration) for each well. We used 1 mM (+)-pentazocine as a non-specific control. Concentrations for non-radioactive (+)-pentazocine in

homologous competition assay were: 100  $\mu\text{M}$ , 10  $\mu\text{M}$ , 1  $\mu\text{M}$ , 100 nM, 10 nM, 1 nM, and 0.1 nM in EBSS with 10% DMSO. Total binding was determined with 1% DMSO vehicle (final concentration). All compound dilutions were tested in triplicate, and samples were incubated for 120 min at room temperature. The reactions were terminated by filtration through PerkinElmer Uni Filter-96 GF/B, presoaked in 0.05% PEI for 120 min, and the 96-well filter plates were counted in PerkinElmer MicroBeta Microplate Counter as described (Yano et al., 2018) with counter efficiency at 31% for [ $^3\text{H}$ ]-(+)-pentazocine.  $K_d$  and  $B_{\text{max}}$  values were determined from at least three independent experiments.

## Bioluminescence Resonance Energy Transfer (BRET) Assay

Drug-induced BRET is conducted as optimized previously (i.e., transfection and experimental conditions) (Urizar et al., 2011; Yano et al., 2018). Briefly, cells were prepared in 96-well plates. 5  $\mu\text{M}$  coelenterazine h was added to each well. Three minutes after addition of coelenterazine h (Nanolight), ligands [(+)-pentazocine (Sigma), PD 144418 (Tocris), and haloperidol (Tocris)] were added to each well in serial dilution. BRET was measured as a ratio between measurements at 535 nm for fluorescence (gain 2500, interval time 0.9) and at 485 nm for luminescence (gain 2500, interval time 0.9) using a PHERastar FSX reader (BMG). Results are calculated for the BRET change (BRET ratio for the corresponding drug minus BRET ratio in the absence of the drug).  $E_{\text{max}}$  values are expressed as the basal subtracted BRET change in the dose-response graphs.

## Animals

Wildtype (WT) C57BL/6J mice were used for  $\sigma\text{1R}$  detection in western blot experiments. Animals were housed with food and water available *ad libitum* in temperature ( $22 \pm 2^\circ\text{C}$ )- and humidity ( $45 \pm 5\%$ )-controlled rooms and were maintained on a 12 h light/dark cycle (lights on: 7:00 a.m.–7:00 p.m.). They were experimentally naive at the start of the study and were maintained in accordance with NIH guidelines. All studies were approved by the Institutional Care and Use Committee of the Intramural Research Program, National Institute on Drug Abuse.

## Statistical Analysis

Statistical analyses were performed using GraphPad Prism version 7.0 (GraphPad Software, San Diego, CA, United States). For **Figures 2C,F,I, 4C,F**, the statistical comparison was obtained by one-way ANOVA followed by *post hoc* Tukey analysis ( $*p < 0.05$ ,  $**p < 0.01$ ,  $***p < 0.005$ , and  $****p < 0.001$ ).

## RESULTS

### The Unmodified WT Shows Distinct Bands up to Densities Corresponding to Octamers

In this study, we used an antibody-based western blot (WB) approach to detect the configurational changes of  $\sigma\text{1R}$  oligomerization in response to ligand binding and to

the modification of the N- or C-terminus. To exclude the confounding effects of endogenous  $\sigma\text{1R}$ , we heterologously expressed (i.e., rescued) various  $\sigma\text{1R}$  constructs in  $\sigma\text{1R}$ -null ( $\Delta\sigma\text{1R}$ ) HEK293T cells (see section “Materials and Methods”).

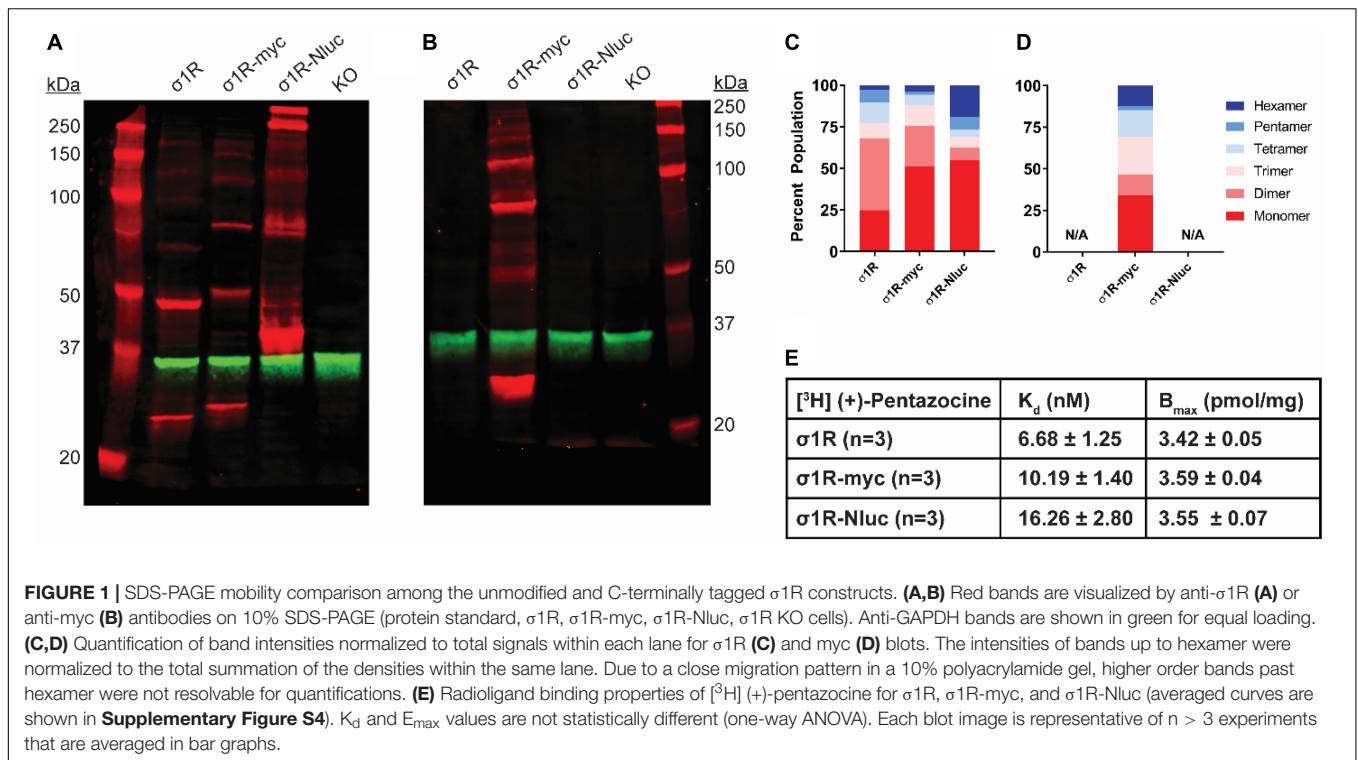
In WB assays, samples would typically be heated, often boiled, in a reducing buffer condition to allow efficient epitope interaction with an antibody in the following step. Indeed, the samples in previous WB assays of  $\sigma\text{1R}$  have also been subjected to heating (Gromek et al., 2014; Tsai et al., 2015; Sambo et al., 2017), unless using the native gel approach (Yano et al., 2018). In this study, we found that by keeping samples on ice before running them on sodium dodecyl sulfate–polyacrylamide gel electrophoresis (SDS-PAGE), we could observe strong-enough signals for homomeric  $\sigma\text{1R}$  interactions when using  $>5 \mu\text{g}$  plasmid DNA per 10-cm plate in transfection (**Supplementary Figure S1D**). Compared to samples receiving boiling treatment ( $100^\circ\text{C}$ ) that resulted in a single monomer band ( $\sim 25 \text{ kDa}$ ), the samples kept on ice showed a unique ladder-like pattern that corresponds to distinct bands from a monomer up to an octamer ( $\sim 200 \text{ kDa}$ ) of  $\sigma\text{1R}$  in WB (**Supplementary Figure S2A**). As expected, none of the bands were observed in the untransfected  $\Delta\sigma\text{1R}$  cells (**Figure 1A**). Therefore, we used the on-ice condition ( $4^\circ\text{C}$ ) for the rest of this study unless otherwise noted.

Using the same protocol, the extent of  $\sigma\text{1R}$  homomeric interactions at the endogenous expression level was tested in brain cortex preparation from mice. Notably, tetramer band has the highest intensity while dimer and very weak monomer densities are observed (**Supplementary Figure S2C**). Therefore, despite the differences in higher order bands compared to the HEK293T heterologous expression, the oligomerization of endogenously expressed  $\sigma\text{1R}$  can be detected by this protocol.

In addition to the B-5 (Santa Cruz)  $\sigma\text{1R}$  antibody, we chose three other commercially available  $\sigma\text{1R}$  antibodies based on their disparate target epitopes (**Supplementary Table S1** and **Supplementary Figures S1A–C**). We compared the capabilities of these antibodies to detect distinct  $\sigma\text{1R}$  oligomer bands in our assay conditions. Similar to B-5, D4J2E (Cell Signaling; **Supplementary Figure S1C**) antibodies also showed a unique ladder-like pattern but not as distinct as B-5.

### The C-Terminally Tagged Constructs Show Distinct Oligomer Bands as Well

Previous reports suggest that C-terminal tagging of  $\sigma\text{1R}$  does not interfere with localization and function of  $\sigma\text{1R}$  (Hayashi and Su, 2003, 2007; Sambo et al., 2017). In addition to our previous  $\sigma\text{1R}$  construct used in the BRET assay in which Nluc is attached to the C-terminus ( $\sigma\text{1R}$ -Nluc) (Yano et al., 2018), to test the C-terminal tagging's effect on the  $\sigma\text{1R}$ - $\sigma\text{1R}$  interaction, we also generated the  $\sigma\text{1R}$ -myc construct, which has a shorter tag at the C-terminus. Both  $\sigma\text{1R}$ -Nluc and  $\sigma\text{1R}$ -myc exhibit ladder-like patterns similar to the unmodified WT  $\sigma\text{1R}$ ; the bands range from  $\sim 26 \text{ kDa}$  (monomer) to  $\sim 208 \text{ kDa}$  (octamer) for  $\sigma\text{1R}$ -myc and  $\sim 44 \text{ kDa}$  (monomer) to  $\sim 352 \text{ kDa}$  (octamer) for  $\sigma\text{1R}$ -Nluc (**Figure 1A**). To confirm the same mobility and density of the bands visualized by an antibody targeting a different epitope, the anti-myc antibody



was used against  $\sigma$ 1R-myc as well. In this WB, the bands are generally brighter, which may indicate a stronger epitope affinity of the anti-myc antibody than that of the anti- $\sigma$ 1R antibody (**Figure 1B**).

To quantify the distribution of  $\sigma$ 1R in each oligomeric population for each condition, we measured the intensity of each band (see section “Materials and Methods”). Similar patterns were observed across the unmodified and C-terminally tagged constructs (**Figures 1C,D**). The higher-order bands (i.e., tetramer, pentamer, and hexamer), which are larger than the trimer revealed by the  $\sigma$ 1R crystal structures (Schmidt et al., 2016), are more intense for  $\sigma$ 1R-Nluc and  $\sigma$ 1R-myc than the unmodified construct (**Figure 1C**).

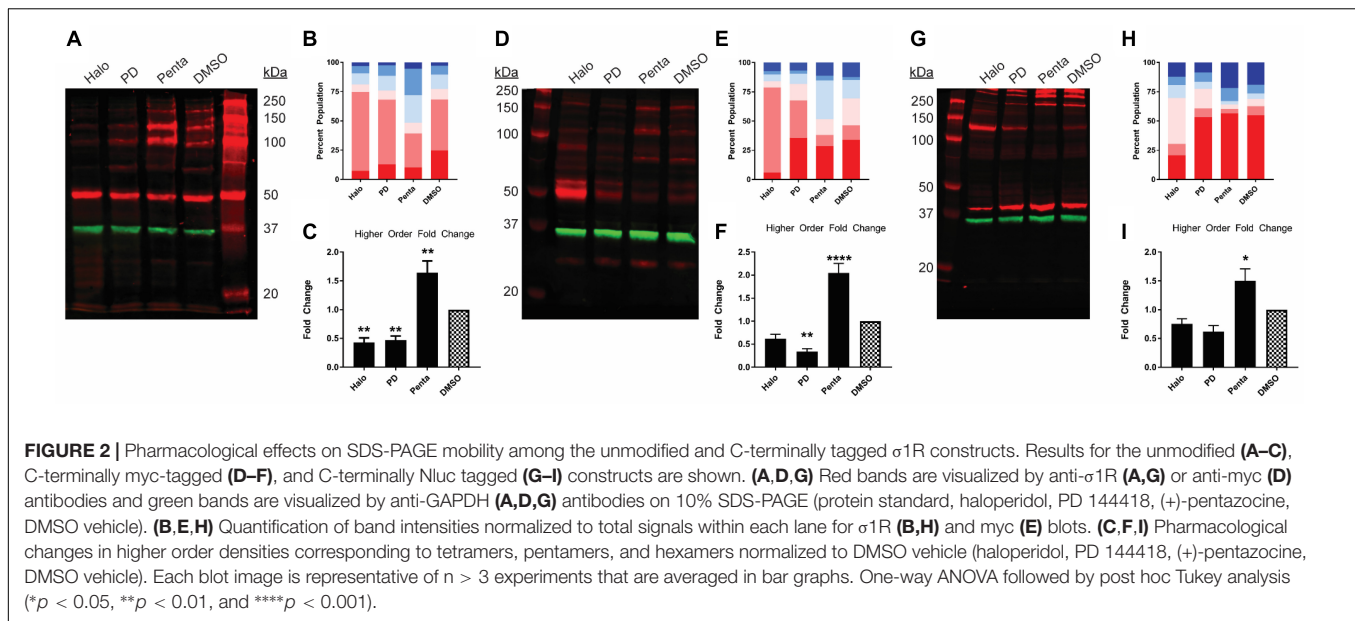
To confirm that the integrity of the ligand binding site and likely the C-terminal domain of the  $\sigma$ 1R constructs are not affected by tagging or the WB condition, radioligand binding assay was conducted with [<sup>3</sup>H](+)-pentazocine. Under the same conditions as the WB (i.e., transfection and protein input), the unmodified and C-terminally-tagged constructs have virtually the same expression levels and similar K<sub>d</sub> (**Figure 1E** and **Supplementary Figure S4**).

## The Unmodified WT and C-Terminally Tagged Constructs Show Similar Extents of Pharmacological Changes in Higher-Order Bands

Previously, we have found that  $\sigma$ 1R undergoes ligand-induced changes of the oligomerization states (Yano et al., 2018). Here, we investigated the effect of ligand binding on the

migration pattern in WB.  $\sigma$ 1R ligands were added to  $\sigma$ 1R-expressing cells and incubated for 1 h before proceeding to sample preparation. 1 h incubation time was chosen to be consistent with the radioligand binding and BRET studies. For unmodified WT  $\sigma$ 1R, both haloperidol and PD144418 decreased the intensities of the higher-order bands (i.e., tetramer, pentamer, and hexamer), while (+)-pentazocine increased their intensities (**Figures 2A–C**). The opposing effects of these ligands are consistent with our previous findings using BRET assays that categorized haloperidol, PD144418, and 4-PPBP into haloperidol-like ligands and (+)-pentazocine and PRE-084 into pentazocine-like ligands (Yano et al., 2018). Consistently, both  $\sigma$ 1R-myc and  $\sigma$ 1R-Nluc showed similar extents of changes in the higher-order bands, in which haloperidol and PD144418 decreased and (+)-pentazocine increased the relative densities of the higher-order bands (**Figures 2D–I**).

In contrast to samples prepared on ice, in the absence of any ligand, temperature increases in the sample buffer decreased the densities of the dimer and above bands, indicating that  $\sigma$ 1R- $\sigma$ 1R interaction is disrupted by the high temperature (**Supplementary Figure S2A**), which was also observed when the experiments were carried out with mouse cortex preparation (**Supplementary Figure S2C**). In the presence of different ligands, the 70°C treatment completely monomerized  $\sigma$ 1R as well, while the monomer densities across different ligand treatments are similar (**Supplementary Figure S2B**). Thus, the  $\sigma$ 1R expression level is unlikely changed by the ligands, because changes in the total copy number would affect monomer band density.



## The N-Terminally Tagged myc- $\sigma$ 1R and Nluc- $\sigma$ 1R Exhibit Very Weak Higher Order Bands

As opposed to the C-terminal tagging, it has been reported that N-terminal tagging of  $\sigma$ 1R interferes with the localization of  $\sigma$ 1R (Hayashi and Su, 2003). To study the effect of N-terminal tagging on the gel mobility of  $\sigma$ 1R, in addition to our previously studied Nluc- $\sigma$ 1R (Yano et al., 2018), we generated the myc- $\sigma$ 1R construct. In our WB assay, using anti- $\sigma$ 1R antibody, the higher-order bands for both myc- $\sigma$ 1R and Nluc- $\sigma$ 1R have much less relative distributions than the unmodified construct (Figures 3A,C). When incubated with anti-myc antibody, the fraction of total density that was present in higher-order bands for myc- $\sigma$ 1R did not notably improve (Figures 3B,D). For Nluc- $\sigma$ 1R the reduced intensities in higher-order bands, are more apparent when compared to the density distribution of the C-terminally tagged  $\sigma$ 1R-Nluc (Figures 1A,C, 3A,C). Even though the oligomerization states are drastically different from their corresponding C-terminal tagged constructs, radioligand binding results showed  $K_d$  and  $B_{max}$  are not significantly different from those of the unmodified construct (Figure 3E and Supplementary Figure S4).

## The N-Terminally Tagged Constructs Show Substantially Different Pharmacology From Unmodified WT $\sigma$ 1R

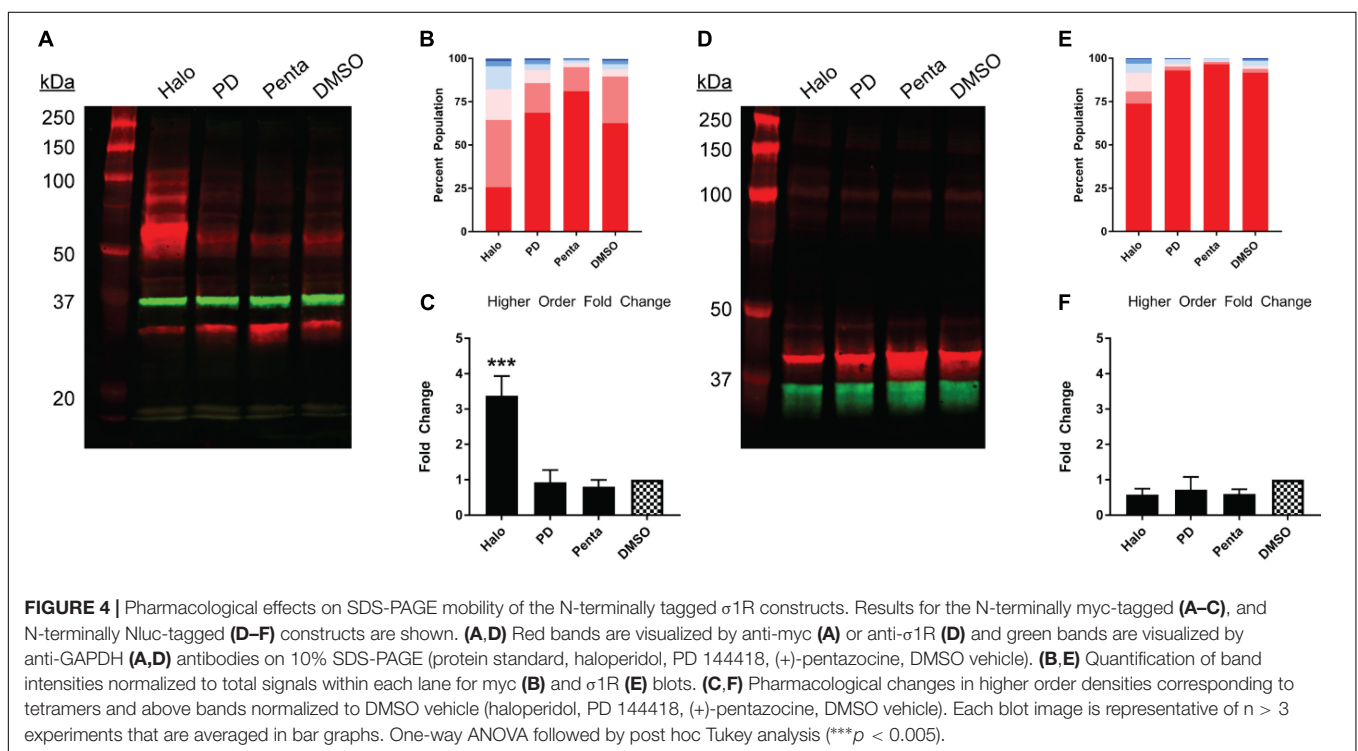
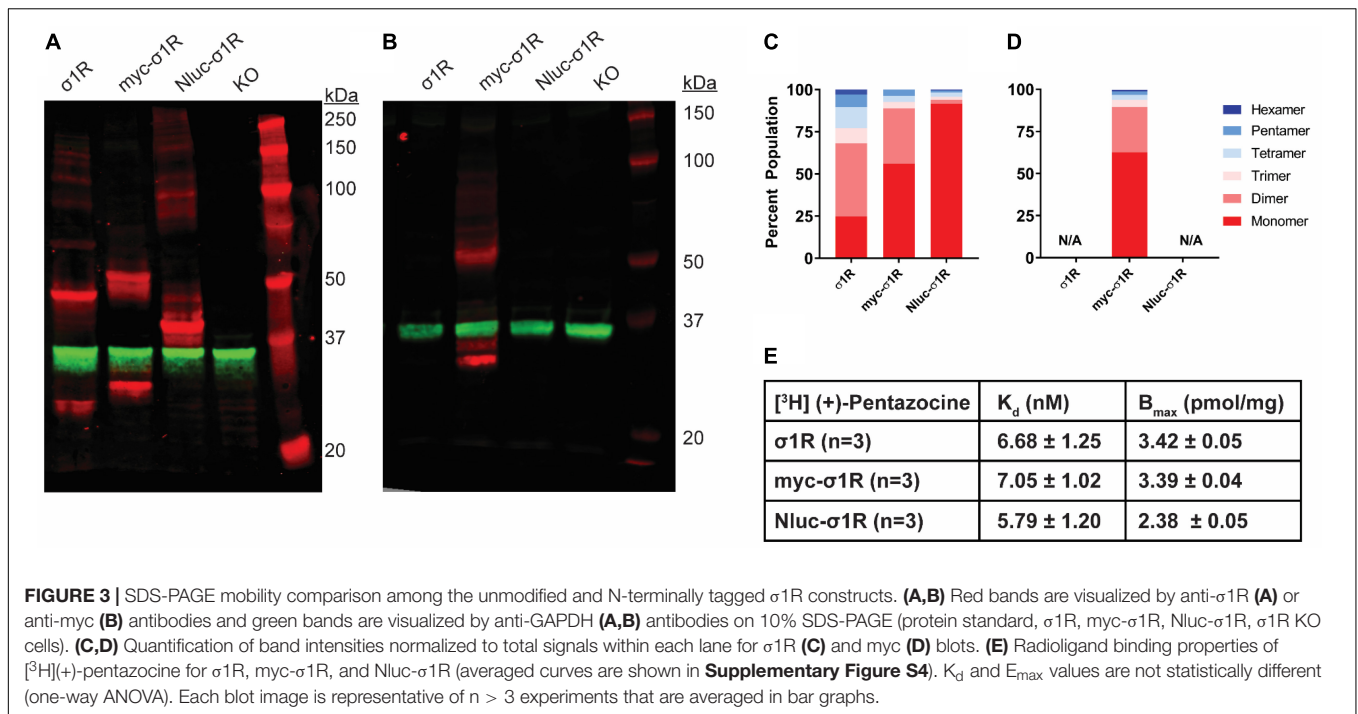
Next, we studied the pharmacology of myc- $\sigma$ 1R and Nluc- $\sigma$ 1R in gel mobility to assess the effects by short and long N-terminal tagging. For myc- $\sigma$ 1R, haloperidol increased the higher-order bands while it diminished the monomer band (Figures 4A–C). PD144418 did not affect the relative density of each band, compared to the DMSO vehicle treated sample. (+)-pentazocine decreased the intensities of higher-order bands while

increasing that of the monomer band. For Nluc- $\sigma$ 1R, haloperidol increased the higher order bands slightly while PD144418 showed effectively no change. (+)-pentazocine showed an increased monomer band (Figures 4D–F). Overall, the pharmacology of myc- $\sigma$ 1R and Nluc- $\sigma$ 1R are similar, i.e., haloperidol increased the densities of higher-order bands, while (+)-pentazocine increased that of monomer bands. However, these pharmacological trends are opposite to that of the unmodified  $\sigma$ 1R (Figures 2A–C), indicating that the N-terminal tagging may interfere with how ligand binding propagates the conformational changes within  $\sigma$ 1R or directly interferes with the formation of oligomers.

## DISCUSSION

Sigma 1 receptor has been extensively studied at molecular level using biochemical and pharmacological approaches (Hayashi and Su, 2007; Narayanan et al., 2011; Gromek et al., 2014; Katz et al., 2016; Romero et al., 2016; Nguyen et al., 2017; Mavlyutov et al., 2018). In this study, we investigated the effects of terminal tagging on  $\sigma$ 1R oligomerization and pharmacology, and revealed the ability of N-terminal modification to interfere with the oligomerization of  $\sigma$ 1R.

Sodium dodecyl sulfate–polyacrylamide gel electrophoresis WB is one of the most commonly used biochemical assays to quantify protein density. Because of detergent solubilization, protein-protein interactions in their native cellular environment can be disrupted in many instances. Here, however, by maintaining samples on ice, we were able to preserve homomeric  $\sigma$ 1R- $\sigma$ 1R interactions and visualize discrete bands corresponding to oligomers as large as octamers by using an antibody (B-5) targeting an epitope at residues 136–169 of  $\sigma$ 1R. As a technical note, after the antibody has been stored for a long time, the antibody staining becomes dimmer and the higher-order bands cannot be visualized, potentially due



to degradation (**Supplementary Figures S1E,F**). Interestingly, the other antibodies against distinct epitopes from different vendors resulted in different visualization patterns indicating the corresponding epitopes may be differentially exposed in different oligomerization states, while residue 136-169 might always be exposed. Although intriguing, these antibodies were

not further pursued because of their significantly lower band intensities, which could be due to insufficient epitope affinities. In general, the WB method described herein is deemed useful to study  $\sigma$ 1R pharmacology since ligand-induced conformational changes, particularly in higher-order bands, can be quantitatively evaluated. Nevertheless, we could not exclude the possibility

that  $\sigma$ 1R-interacting proteins may co-migrate with  $\sigma$ 1R and result in some of the observed bands, though such contribution is likely minimal given the significantly higher heterologous expression level of  $\sigma$ 1R compared to the other endogenous proteins in this study.

We have previously reported a BRET-based proximity assay to study  $\sigma$ 1R pharmacology in HEK293T cells (Yano et al., 2018). The C-terminally tagged  $\sigma$ 1R-Nluc construct used in that study showed a similar response to ligands in the migration pattern of higher-order bands as the unmodified  $\sigma$ 1R, demonstrating that BRET responses very likely reflect the configurational changes in  $\sigma$ 1R oligomerization observed in the unmodified  $\sigma$ 1R. In current study, we used  $\Delta\sigma$ 1R HEK293T cells. By repeating the BRET experiment in  $\Delta\sigma$ 1R HEK293T cells transfected with  $\sigma$ 1R-Nluc and  $\sigma$ 1R-Venus (**Supplementary Figure S3**), we found the  $\sigma$ 1R pharmacology effectively remained the same as the previously reported BRET results in HEK293T cells (Yano et al., 2018). Given that in the BRET assays, haloperidol and PD144418 increased BRET signals while in the WB assays, they decreased higher-order band densities and increased lower-order band densities, we speculate that the BRET readouts recapitulate the changes in the lower-order populations. In that regard, the dimer and trimer populations comprise 48.9% in haloperidol and 24.3% in PD144418, compared to 13.7% in DMSO (**Figure 2H**). The pattern can be correlated with the BRET<sub>max</sub> order, in which haloperidol shows higher BRET<sub>max</sub> than PD144418 (**Supplementary Figure S3**).

We observed that the total signal (i.e., summation of band densities up to hexamer) increased with (+)-pentazocine (38%) and decreased with haloperidol (−25%) or PD144418 (−23%) compared to DMSO lane (**Figure 2A**). Since there is no change in  $\sigma$ 1R expression level across different ligand conditions (**Supplementary Figure S2B**), these changes in total signal, primarily due to changes in the higher-order bands, are caused by changes in either the copy number and/or changes in epitope accessibility in higher-order oligomers. If there is an increase in copy number of  $\sigma$ 1R in higher order bands, the increased populations should equal the collective decrease in lower-order bands. However, as we only observed a weak complementary decrease in lower-order bands, in addition to increased copy number, we postulate that changes in the epitope affinity in higher-order populations of  $\sigma$ 1R plays a role in increased higher-order band intensities as well.

In addition, we found that the N-terminal modification limits higher-order interactions of  $\sigma$ 1R in our solubilization condition, consistent with the previously reported detrimental effects of N-terminal tagging or point mutation on the cellular localization and function (Hayashi and Su, 2003). It is noteworthy that there is a putative Arg-Arg ER retention signal (Michelsen et al., 2005) at the N-terminus of  $\sigma$ 1R. We propose that the steric hindrance of the N-terminally tagged protein may interfere with the recognition of Arg-Arg tandem residues at the seventh and eighth positions. This interference is potentially akin to some other membrane proteins that escape from ER retention due to its Arg-Arg motif masked by nearby domains [e.g., GABA<sub>B</sub> receptor (Frangaj and Fan, 2018)]. Despite its probable mislocalization, the folding of  $\sigma$ 1R is likely only be modestly affected by

the N-terminal tagging, considering the similar binding  $K_d$  compared to that of the unmodified construct. Therefore, the reduced  $\sigma$ 1R- $\sigma$ 1R interaction may arise from the membrane environment in which  $\sigma$ 1R is localized such that the  $\sigma$ 1R density may be too low to find an interacting partner. Further, while the exterior of the barrel motif of the C-terminal domain has been revealed by the crystal structures to be the interface for trimer, it is likely other part of the of the protein involves in forming other oligomer states, such as the N-terminus and N-terminal transmembrane helix<sup>1</sup>, which may be disrupted by the N-terminal tagging.

## DATA AVAILABILITY STATEMENT

All datasets generated for this study are included in the article/**Supplementary Material**.

## ETHICS STATEMENT

The animal study was reviewed and approved by the Institutional Care and Use Committee of the Intramural Research Program, National Institute on Drug Abuse.

## AUTHOR CONTRIBUTIONS

HY and LS designed the study. LL, SN, and HY performed the experiments. All authors took part in interpreting the results. HY wrote the initial draft, with LL and LS participating in revising the manuscript.

## FUNDING

Support for this research was provided by the National Institute on Drug Abuse – Intramural Research Program, Z1A DA000606-03 (LS).

## ACKNOWLEDGMENTS

We would like to thank Drs. Yoki Nakamura, Yuriko Kimura, and Tsung-Ping Su at NIDA for collaborating with us to develop  $\Delta\sigma$ 1R HEK293T cells used in this assay, preparing the cortex tissue samples from mice, and sharing their image detection instrument (LI-Cor). We also thank Dr. Andrew Fant for insightful discussions.

## SUPPLEMENTARY MATERIAL

The Supplementary Material for this article can be found online at: <https://www.frontiersin.org/articles/10.3389/fnins.2019.01356/full#supplementary-material>

<sup>1</sup>Abramyan, A. M., Yano, H., Xu, M., Liu, L., Naing, S., Fant, A. D., et al. (Submitted). *The Mutation of Glu102 Disrupts Higher-Order Oligomerization of the Sigma 1 Receptor*.

## REFERENCES

- Frangaj, A., and Fan, Q. R. (2018). Structural biology of GABAB receptor. *Neuropharmacology* 136, 68–79. doi: 10.1016/j.neuropharm.2017.10.011 doi: 10.1016/j.neuropharm.2017.10.011
- Gromek, K. A., Suchy, F. P., Meddaugh, H. R., Wrobel, R. L., LaPointe, L. M., Chu, U. B., et al. (2014). The oligomeric states of the purified sigma-1 receptor are stabilized by ligands. *J. Biol. Chem.* 289, 20333–20344. doi: 10.1074/jbc.M113.537993
- Hayashi, T., and Su, T. P. (2003). Sigma-1 receptors (sigma(1) binding sites) form raft-like microdomains and target lipid droplets on the endoplasmic reticulum: roles in endoplasmic reticulum lipid compartmentalization and export. *J. Pharmacol. Exp. Ther.* 306, 718–725. doi: 10.1124/jpet.103.051284
- Hayashi, T., and Su, T. P. (2007). Sigma-1 receptor chaperones at the ER-mitochondrion interface regulate Ca(2+) signaling and cell survival. *Cell* 131, 596–610. doi: 10.1016/j.cell.2007.08.036
- Katz, J. L., Hiranita, T., Hong, W. C., Job, M. O., and McCurdy, C. R. (2017). A role for sigma receptors in stimulant self-administration and addiction. *Handb. Exp. Pharmacol.* 244, 177–218. doi: 10.1007/164\_2016\_94
- Katz, J. L., Hong, W. C., Hiranita, T., and Su, T. P. (2016). A role for sigma receptors in stimulant self-administration and addiction. *Behav. Pharmacol.* 27, 100–115. doi: 10.1097/FBP.0000000000000209
- Maurice, T., and Su, T. P. (2009). The pharmacology of sigma-1 receptors. *Pharmacol. Ther.* 124, 195–206. doi: 10.1016/j.pharmthera.2009.07.001
- Mavylutov, T., Chen, X., Guo, L., and Yang, J. (2018). APEX2- tagging of Sigma 1-receptor indicates subcellular protein topology with cytosolic N-terminus and ER luminal C-terminus. *Protein Cell* 9, 733–737. doi: 10.1007/s13238-017-0468-5
- Michelsen, K., Yuan, H., and Schwappach, B. (2005). Hide and run. Arginine-based endoplasmic-reticulum-sorting motifs in the assembly of heteromultimeric membrane proteins. *EMBO Rep.* 6, 717–722.
- Narayanan, S., Bhat, R., Mesangeau, C., Poupaert, J. H., and McCurdy, C. R. (2011). Early development of sigma-receptor ligands. *Future Med. Chem.* 3, 79–94. doi: 10.4155/fmc.10.279
- Nguyen, L., Lucke-Wold, B. P., Mookerjee, S., Kaushal, N., and Matsumoto, R. R. (2017). Sigma-1 receptors and neurodegenerative diseases: towards a hypothesis of sigma-1 receptors as amplifiers of neurodegeneration and neuroprotection. *Adv. Exp. Med. Biol.* 964, 133–152. doi: 10.1007/978-3-319-50174-1\_10
- Romero, L., Merlos, M., and Vela, J. M. (2016). Antinociception by sigma-1 receptor antagonists: central and peripheral effects. *Adv. Pharmacol.* 75, 179–215. doi: 10.1016/bs.apha.2015.11.003
- Sambo, D. O., Lin, M., Owens, A., Lebowitz, J. J., Richardson, B., Jagarine, D. A., et al. (2017). The sigma-1 receptor modulates methamphetamine dysregulation of dopamine neurotransmission. *Nat. Commun.* 8:2228. doi: 10.1038/s41467-017-02087-x
- Schmidt, H. R., Betz, R. M., Dror, R. O., and Kruse, A. C. (2018). Structural basis for sigma1 receptor ligand recognition. *Nat. Struct. Mol. Biol.* 25, 981–987. doi: 10.1038/s41594-018-0137-2
- Schmidt, H. R., Zheng, S., Gurpinar, E., Koehl, A., Manglik, A., and Kruse, A. C. (2016). Crystal structure of the human sigma1 receptor. *Nature* 532, 527–530. doi: 10.1038/nature17391
- Su, T. P., Su, T. C., Nakamura, Y., and Tsai, S. Y. (2016). The sigma-1 receptor as a pluripotent modulator in living systems. *Trends Pharmacol. Sci.* 37, 262–278. doi: 10.1016/j.tips.2016.01.003
- Tsai, S. Y., Chuang, J. Y., Tsai, M. S., Wang, X. F., Xi, Z. X., Hung, J. J., et al. (2015). Sigma-1 receptor mediates cocaine-induced transcriptional regulation by recruiting chromatin-remodeling factors at the nuclear envelope. *Proc. Natl. Acad. Sci. U.S.A.* 112, E6562–E6570. doi: 10.1073/pnas.1518894112
- Urizar, E., Yano, H., Kolster, R., Gales, C., Lambert, N., and Javitch, J. A. (2011). CODA-RET reveals functional selectivity as a result of GPCR heteromerization. *Nat. Chem. Biol.* 7, 624–630. doi: 10.1038/nchembio.623
- Weissman, A. D., Su, T. P., Hedreen, J. C., and London, E. D. (1988). Sigma receptors in post-mortem human brains. *J. Pharmacol. Exp. Ther.* 247, 29–33.
- Yano, H., Bonifazi, A., Xu, M., Guthrie, D. A., Schneck, S. N., Abramyan, A. M., et al. (2018). Pharmacological profiling of sigma 1 receptor ligands by novel receptor homomer assays. *Neuropharmacology* 133, 264–275. doi: 10.1016/j.neuropharm.2018.01.042

**Conflict of Interest:** The authors declare that the research was conducted in the absence of any commercial or financial relationships that could be construed as a potential conflict of interest.

Copyright © 2019 Yano, Liu, Naing and Shi. This is an open-access article distributed under the terms of the Creative Commons Attribution License (CC BY). The use, distribution or reproduction in other forums is permitted, provided the original author(s) and the copyright owner(s) are credited and that the original publication in this journal is cited, in accordance with accepted academic practice. No use, distribution or reproduction is permitted which does not comply with these terms.